Imaging of porphyrin-specific fluorescence in pathogenic bacteria *in vitro* using a wearable, hands-free system

Junhong Sun[1,#], Sangeevan Vellappan[1,2,#], Johnathan Akdemir[2], Liviu Steier[3], Richard E. Feinbloom[4,5], Srujana S. Yadavalli[1,2]*

[1]Waksman Institute of Microbiology, Rutgers University, Piscataway, NJ USA

[2]Department of Genetics, School of Arts and Sciences, Rutgers University, Piscataway, NJ USA

[3]Department of Preventive and Restorative Sciences, Robert Schattner Center, School of Dental Medicine, University of Pennsylvania, Philadelphia, PA USA

[4]Designs for Vision, Inc., Bohemia, NY USA

[#]These two authors contributed equally to this work

*Corresponding author

Waksman Institute of Microbiology

Rutgers University

190 Frelinghuysen Rd

Piscataway NJ 08854

Phone: 848-445-0251

Email: sam.yadavalli@rutgers.edu

Short title: Porphyrin-specific fluorescence in pathogenic bacteria

Keywords: Bacteria, porphyrins, fluorescence, fluorescence imaging, wearable technology

Highlights

- Fluorescence imaging detects porphyrins in bacteria via natural fluorescence.
- A lightweight, hands-free device enables rapid, non-invasive clinical assessments.
- The study tested 15 bacterial and 2 fungal strains for porphyrin-based autofluorescence.
- 14 bacteria fluoresced on Porphyrin Test Agar, 9 on blood agar plates.
- The REVEAL system aids in diagnosing infections and guiding real-time treatments.

Abstract

Fluorescence imaging is an effective method for detecting porphyrin production in bacteria, leveraging the natural fluorescence properties of porphyrins. Here we use a simple, lightweight, hands-free device for rapid, non-invasive assessments in clinical settings, microbial research, and diagnostic applications. Specifically in this study, we examined 15 bacterial and 2 fungal strains commonly associated with skin, oral, and/or multi-site infections at wound sites for their ability to autofluoresce based on their porphyrin production. We utilized Remel Porphyrin Test Agar and blood agar plates to monitor red fluorescence over several days of growth under aerobic or anaerobic conditions using the wearable REVEAL FC imaging system with a 405 nm violet excitation headlight paired with eyewear carrying 430 nm emission lenses. Fourteen of the fifteen bacteria produced red fluorescence when grown on Porphyrin Test Agar and nine of the fifteen bacteria also displayed red fluorescence on blood agar plates, consistent with their ability to synthesize porphyrins. Taken together, our results elucidate the sensitivity, effectiveness, and convenience of using wearable technology to detect pathogens that produce porphyrin-specific fluorescence. Consequently, the REVEAL system has immense potential to help diagnose wound infections, direct clinical procedures, and guide treatment options in real-time using fluorescence imaging all while minimizing the risk of contamination.

1. Introduction

Microbial infections pose significant threats, especially in wound healing (1, 2). If ignored or not treated promptly, the infection may advance from initial contamination to colonization, local infection, and even systemic infection, potentially leading to severe conditions like sepsis and multiple organ dysfunction syndrome (2). In cases such as the infection in diabetic foot ulcers, timely detection is crucial to prevent potential complications like amputation (3). Similarly, disregarding the initial stages of dental plaque accumulation in the oral cavity can trigger oral health complications, such as gingivitis, periodontitis, dental caries, and even tooth loss (4). Notably, approximately 47.2% of individuals aged 30 years and older are affected by some form of periodontal disease (4).

Considering the rapid spread of infections, when possible, timely detection and effective management are crucial to prevent infections from progressing to severe stages and reduce the risk of complications, such as tissue necrosis and the need for amputation (5, 6). Traditional methods of detecting and confirming bacterial infections, such as culturing and susceptibility testing, are laborious and time-consuming, taking days to yield results (7). In recent years, there has been a development of fluorescence-based approaches for real-time visualization of intrinsic fluorescence from porphyrins produced in bacteria in wound sites and oral plaques, enabling earlier detection (8–11). Fluorescence-based detection of bacteria relies on the production of porphyrins, a crucial metabolic intermediate essential for heme biosynthesis and various biological processes (12). Heme, synthesized by pathogens or obtained from host sources during infection, plays a pivotal role in energy generation through the electron transport chain (12). Heme biosynthesis is vital to both aerobic and anaerobic respiration in prokaryotes (13). In laboratory settings, heme precursors can be provided to microorganisms through specialized media like porphyrin test agar, or blood agar enriched with 5% sheep's blood cells

76 (14, 15). As pathogens synthesize porphyrins, exposure to violet light (~400-450 nm) leads to
77 their excitation, emitting light at distinct wavelengths within the red fluorescence at 620-630 nm
78 (16, 17). Like porphyrin, pyoverdines are siderophores uniquely produced by *Pseudomonas*
79 *spp.* for iron acquisition, which can be visualized in cyan spectral bands (18). This fluorescence
80 emission facilitates identifying and visualizing pathogens, thereby enhancing diagnostic
81 procedures.
82
83 Currently, the real-time fluorescence-guided detection of pathogens uses a handheld device (8).
84 Serena and colleagues suggest that the use of fluorescence imaging has resulted in changes to
85 69% of the treatment plans and most importantly, there has been a significant improvement in
86 patient care in 90% of study wounds (19). This comes as a great benefit to the patient and the
87 clinician. However, as this technology requires a clinician to use both hands, it hampers the
88 clinician's ability to provide treatment during real-time fluorescence visualization. The adoption
89 cost of this technology requires capital expenditure and incurs ongoing operational costs that
90 limit adoption. Hence, there is a need to develop alternative tools to the existing non-wearable
91 methods, which can allow for rapid and non-invasive assessment.
92
93 In this study, we report on a new, wearable/ hands-free fluorescence visualization technology
94 (REVEAL FC wearable imaging system, Design for Vision Inc., Fig 1a) that will enable clinicians
95 to evaluate the infection at the wound site based on real-time visualization of pathogens and
96 simultaneously make active treatment decisions. Specifically, we sought to test and characterize
97 porphyrin detection *via* autofluorescence *in vitro* for some of the common pathogens involved in
98 skin, oral, and other (respiratory, intestinal, urinary tracts, or blood) infections over a period of
99 multiple days. We included 15 bacteria and 2 fungi in our analysis. Our results indicate the
100 ability of REVEAL FC to visualize porphyrin-specific red-orange or pink fluorescence in 14 of the
101 17 strains tested on porphyrin test agar (Fig 1b). Moreover, we also observed a fluorescence

signal for 9 of the 17 strains grown on blood agar plates, suggesting a strong potential for the detection of microbial infections in wound sites in a clinical setting using the REVEAL FC wearable technology.

2. Materials and Methods

2.1. Strains

E. coli K-12 MG1655 strain is from the Yadavalli lab collection. The following strains, *Pseudomonas aeruginosa* PAO1, *Klebsiella pneumoniae* ATCC 13883, *Staphylococcus aureus* USA300_LAC, a community-acquired MRSA strain, and *S. Typhimurium* 14028, were gifts from Drs. Bryce Nickels (Rutgers), Huizhou Fan (Rutgers), Jeffrey Boyd (Rutgers), and Dieter Schifferli (University of Pennsylvania). All other bacterial and fungal strains used in the study were purchased from the American Type Culture Collection (ATCC). See Table S1 for additional details on the bacterial and fungal strains used in this study.

2.2. Media and growth conditions

For routine growth, bacterial and fungal strains were cultured in liquid or solid agar medium, either aerobically or anaerobically depending on the organism as specified in Table S1. Agar plates and culture tubes were then incubated at 37°C with aeration (for aerobic growth) or an anaerobic growth chamber (for anaerobic growth), depending on a given strain's specific growth requirement.

To assess porphyrin production and monitor the associated fluorescence, the strains were streaked out and grown on Remel Porphyrin Test Agar (PTA, Thermo Fisher Scientific), and/or blood agar (BA, tryptic soy agar with 5% sheep blood, Thermo Fisher Scientific). Note that both PTA and BA plates contain heme precursors. For strains grown aerobically, PTA and BA plates

were incubated for 5 days at 37°C. Plates were pulled out for imaging daily and returned to incubation until day 5. For anaerobic strains, PTA and BA plates were incubated for 10 days in the anaerobic growth chamber, including one plate per strain for each time point (days 2, 4, 7, and 10) to be pulled out for imaging. At the indicated time points, plates were imaged using the REVEAL FC technology as described below.

2.3. Fluorescence imaging

For strains grown aerobically, imaging was performed daily from day 1 to 5. For strains grown in the anaerobic chamber, one plate corresponding to each strain was removed from the chamber on days 2, 4, 7, and 10, and imaged. Fluorescence visualization and imaging were performed using the REVEAL FC, a wearable system equipped with the following: a 405 nm headlight for excitation, an observational eyewear with an emission filter at 430 nm, a rechargeable power pack (2 included) with 9 hours of runtime per pack, a smart device attachment for simple and easy documentation. For this study, a smartphone adapter with a 430 nm emission filter was attached to an Apple iPhone 12 to capture the images. The images were taken in a dark room. Images were analyzed and processed using ImageJ (20).

3. Results

3.1. REVEAL FC imaging system for *in vitro* visualization and imaging of microbial fluorescence

Fluorescence visualization requires an excitation source and an emission filter to eliminate the excitation illumination to maximize the observation of the fluorescent response. The REVEAL FC developed by Designs for Vision Inc. is a wearable system that is composed of a headlight that provides excitation and observational eyewear that includes the emission filter (Fig 1). It is well documented that porphyrins fluoresce when exposed to light in the 400-409nm range (21).

152 Porphyrins are produced as by-products by several microorganisms, including pathogens of
153 interest. The REVEAL FC headlight utilizes an LED at 405 nm wavelength. Even though the
154 peak of this LED is at 405nm, well within the excitation range of porphyrins, LEDs are relatively
155 unfocused. The LED has a wide spectral bandwidth with a transmission range (~380 – 450 nm)
156 that is too broad for specific excitation of porphyrins (Fig S1) and the spot is too wide to respond
157 to lensing. The REVEAL FC system uses proprietary and patented technology involving short
158 wave pass edge filters (shortpass filters) to narrow the spectral bandwidth. Focusing the energy
159 of the LED to a fixed spot provides uniform illumination within the wavelengths that strongly
160 excite porphyrins (400 – 425 nm) while eliminating unnecessary wavelengths that could inhibit
161 the visualization of the fluorescence response. The emission filter is incorporated into a pair of
162 glasses, which removes all wavelengths less than 430 nm providing a clear image of the field
163 with no tinting. All the excitation light is removed by the emission filter observational glasses
164 allowing maximum visualization of the fluorescence response. For documentation, a
165 smartphone adapter is provided that contains the same emission filter (Fig 1). This is intended
166 to be attached to any smart device to document and capture the fluorescent images.
167

168 **3.2. Porphyrin-specific fluorescence in bacteria and fungi causing skin infection**

169 We explored the fluorescent characteristics of seven prevalent bacterial species and two fungal
170 species known for causing skin infections or thriving on open skin wounds using the REVEAL
171 FC system. Among the bacteria tested, three are Gram-positive (*S. aureus*, *C. minutissimum*, *C.*
172 *acnes*) while the remaining four, *A. hydrophila*, *S. marcescens*, *V. vulnificus* and *P.aeruginosa*
173 are Gram-negative (Table 1). These bacterial strains were grown aerobically except for *C.*
174 *acnes*, which is an obligate anaerobe. All of them demonstrate red fluorescence to different
175 extents as monitored over several days and described below (Table 1, Fig 2).
176

177 In aerobic growth, all bacterial species exhibited fluorescence, while the fungi did not (Table 1,
178 Fig 2a). *Staphylococcus aureus* displayed intense red fluorescence on porphyrin test agar
179 (PTA) from day 1, maintaining its intensity through day 5. No fluorescence was observed on
180 blood agar (BA), whose base is tryptic soy medium (Table S1) that is known to exhibit
181 background fluorescence that can mask the porphyrin-specific signal (8). Through the Boyd lab
182 at Rutgers, we had access to *S. aureus hemB* mutant strain, which is deficient in heme
183 acquisition and porphyrin production (22). Consistently, *S. aureus hemB* mutant showed no
184 fluorescence throughout the five days, serving as a negative control (8). *Serratia marcescens*
185 also showed fluorescence on both PTA where the red fluorescence was visible from day 1,
186 intensifying with each passing day until day 5. On BA, *S. marcescens* seemed to show a faint
187 pink fluorescence on day 1, though there was no signal on days 2 and 5. *Corynebacterium*
188 *minutissimum* exhibited red fluorescence on PTA starting from day 1, with increased intensity on
189 days 2 and 3, persisting at least until day 5 when all colonies exhibited red fluorescence.
190 Interestingly, we detected red fluorescence for *C. minutissimum* on BA from day 1, reaching
191 maximum intensity by days 2-3, which indicates a signal higher than the background for BA and
192 the fluorescence diminished by day 5. Similarly, for *Vibrio vulnificus*, bright red fluorescence was
193 visible on days 1 and 2, gradually diminishing by days 3 and 5. On BA, *V. vulnificus* showed red
194 fluorescence as observed on days 1 and 2, with the intensity decreasing and nearly
195 disappearing by day 5. *Aeromonas hydrophila* displayed red fluorescence on PTA from day 1,
196 intensifying remarkably by day 2 and the bright red signal stayed steady until day 5. Similar to
197 *C. minutissimum* and *V. vunificus*, we observed red fluorescence for *A. hydrophila* on BA but
198 with a delayed appearance on day 2, progressively intensifying by day 5. *Pseudomonas*
199 *aeruginosa* exhibited red fluorescence on PTA, with a weak signal on day 1, transitioning to a
200 brighter red signal by day 2 and continuing into day 5 (Fig 2a). On BA, *P. aeruginosa* exhibited
201 cyan fluorescence on day 1, persisting until day 5. *Pseudomonas spp.* are known to synthesize

202 a variety of phenazine pigments including pyoverdines (23), which contribute to the observed
203 cyan fluorescence in our *P. aeruginosa* PAO1 strain.
204
205 The fluorescence changes in anaerobes were observed over a longer period, extending up to
206 10 days, due to their slower growth rate. *Cutibacterium acnes*, an aerotolerant anaerobe (24),
207 exhibited fluorescence on both PTA and BA (Fig 2b). It displayed red fluorescence from day 2,
208 intensifying by day 4 and reaching peak intensity around day 7, but the fluorescence intensity
209 reduced on day 10. On BA, very faint red fluorescence was observed on day 2, which is more
210 evident on day 4, intensifying by day 7, and diminished by day 10. Fungal strains *Candida*
211 *albicans* and *Malassezia furfur* did not show red fluorescence, which is consistent with previous
212 studies (8) (Fig 2c).
213
214 **3.3. Porphyrin-specific fluorescence in bacteria causing oral infection**
215 We examined two bacterial pathogens known for causing oral infections: *Streptococcus mutans*,
216 a Gram-positive bacterium typically inhabiting dental plaque (25), and *Porphyromonas*
217 *gingivalis*, a Gram-negative obligate anaerobe associated with pulpal infections, oral abscesses,
218 and periodontitis (26). *S. mutans* showed no fluorescence under aerobic growth but appeared to
219 show a faint orange signal under anaerobic conditions (Table 1, Fig 3). The second oral
220 pathogen, *P. gingivalis* formed red colonies on PTA, beginning as early as day 2 and 4, but
221 diminishing by day 7 and becoming less visible by day 10 (Fig 3b). On BA, it exhibited no
222 fluorescence on day 2 but developed red fluorescence by day 4. By day 7 on BA, there is a
223 reduction in the red fluorescence and *P. gingivalis* starts to show black pigmentation, which is
224 more prominent by day 10 (Fig 3b). The black-pigmented colonies on blood agar are associated
225 with the accumulation of heme complexes as noted previously (27).
226
227 **3.4. Porphyrin-specific fluorescence in bacteria causing multi-site/other infections**

228 In this section, we tested six bacterial strains that exhibit a diverse range of pathogenic
229 behaviors across distinct anatomical sites and not being exclusively confined to cutaneous or
230 oral infection (Table 1). Two of the six bacterial strains are Gram-positive, while the remaining
231 four are Gram-negative. Five of these species (*Listeria monocytogenes*, *Escherichia coli*,
232 *Klebsiella pneumoniae*, *Salmonella typhimurium,* and *Proteus mirabilis*) demonstrate
233 fluorescence under aerobic conditions, whereas one (*Streptococcus pyogenes*) exhibits
234 fluorescence exclusively under anaerobic conditions (Fig 4).
235
236 Under aerobic growth conditions, *S. pyogenes*, a facultative anaerobe (28), did not exhibit any
237 fluorescence on PTA (Fig 4a). However, when *S. pyogenes* was grown under anaerobic growth
238 conditions, red fluorescence was readily visible from day 2 and persisted through days 4, 7, and
239 10 on both PTA and BA (Fig 4b). *L. monocytogenes* exhibited fluorescence on PTA from day 1,
240 intensifying by day 2 with a slight reduction in intensity by day 5 (Fig 4a). Three strains, *E. coli*,
241 *K. pneumoniae*, and *S. typhimurium* displayed red fluorescence from day 1 with an increased
242 intensity on day 2, which remained strong and stable through day 5. Intriguingly, *P. mirabilis*
243 exhibited bright pink fluorescence on PTA on day 1, intensifying on days 2 and 3, but reducing
244 in intensity by day 5. On BA, *P. mirabilis* showed cyan fluorescence, which was visible on day 1,
245 gradually intensifying by day 3 and remaining consistent thereafter. Secondary metabolites such
246 as phenazines are thought to be produced by a variety of bacteria (29) and the cyan
247 fluorescence observed here for *P. mirabilis* grown on BA may be due to the accumulation of a
248 pyoverdine-like pigment.
249

250 4. Discussion and conclusions

251 Wearable technology in clinical practice and diagnostics encompasses devices such as
252 smartwatches, fitness trackers, smart clothing, and implantable sensors, which collect data on

253 various physiological parameters such as heart rate, activity levels, sleep patterns, blood
254 glucose levels, and more (30, 31). These devices have a broad scope of applications in
255 monitoring chronic conditions, fitness, wellness, rehabilitation, clinical trials, and mental health
256 as well as early diagnosis and prevention. Additionally, there has been progress in developing
257 wearable devices for clinicians and healthcare professionals ranging from smartwatches and
258 augmented reality glasses to biometric sensors to enhance diagnosis, surgical planning,
259 precision, and hands-free communication (32, 33).
260
261 In this study, we use the REVEAL FC imaging system developed by Designs for Vision Inc., a
262 lightweight and comfortable hands-free device that can be customized to the operator's ocular
263 specifications (Fig 1, S1). It minimizes cross-contamination risks and enhances objective
264 assessment capabilities, overcoming limitations posed by bulky and tedious traditional tools.
265 Here we systematically analyzed 15 bacterial and 2 fungal pathogens (Table 1, S1) for red
266 fluorescence associated with porphyrin production *in vitro* under aerobic (days 1 through 5) or
267 anaerobic (days 2 through 10) growth conditions. By plating strains on porphyrin test agar
268 (PTA), we detected a strong red fluorescent signal in all but one (*S. mutans*) of the bacterial
269 strains tested. *S. pyogenes* displayed red fluorescence but only under anaerobic growth
270 conditions. Two other *Streptococcus* strains do not display red fluorescence as documented
271 previously (8), and some bacteria from this genus are known to be deficient in heme
272 biosynthesis (12, 34). Remarkably, red fluorescence has been reported for *S. mutans* in a
273 dentin caries model pointing to a potential media- and context-dependent mechanism for
274 porphyrin production in this bacterium (35).
275
276 For a majority of the bacterial strains, the signal was evident by day 1 and in a few cases,
277 depending on the individual bacterial strain, there was a delayed onset of fluorescence. We also
278 plated the strains on blood agar and found that 9 of the 15 bacteria displayed red fluorescence.

279 It is worth noting that the trypic soy blood agar medium has background fluorescence that
280 typically masks any signal from the bacteria, however, REVEAL was able to detect the red
281 signal above the threshold of the background, suggesting that this system is highly sensitive.
282 Unsurprisingly, the two fungal strains included in this study, *C. albicans* and *M. furfur* did not
283 show porphyrin-dependent red fluorescence, suggesting that they may not produce heme and
284 instead acquire heme from their environments (36).
285
286 This method, like other porphyrin-based approaches, is limited by the fact that not all bacteria
287 produce porphyrins. Internal and external factors can also impact porphyrin production, affecting
288 detection. While the in vitro agar plate model may not fully replicate real-world infection
289 conditions, it provides a foundational step to guide clinicians.
290
291 Overall, wearable technology for healthcare professionals enhances medical practice by
292 enabling faster detection and intervention, improving patient care, increasing efficiency, and
293 supporting more informed clinical decision-making. The use of wearable technology is directly
294 linked to improved patient outcomes in clinical settings (37). For instance, the detection of
295 bacteria in the oral cavity plays a crucial role in diagnosing and treating infections, as they serve
296 as indicators for infected tissue and dental plaque (15). Previous work has shown that
297 fluorescence imaging using the REVEAL system can help with diagnosis and treatment
298 guidance in cariology, oral hygiene, and peri-implantitis (35, 38–40).
299
300 More broadly, the smart wearable fluorescence imaging system described here has immense
301 potential for diagnosis, treatment, and many other applications across pharmaceutical,
302 healthcare, food, and agricultural industries.
303

Acknowledgement

We thank Drs. Meliza Talaue, Xuesong Zhang, and Dr. Martin Blaser's laboratory at the Center for Advanced Biotechnology and Medicine at Rutgers University for the access and use of an anaerobic chamber.

Funding

This work was supported by funding from different sources - the National Institutes of Health - National Institute of General Medical Sciences (NIH-NIGMS) ESI-MIRA R35 GM147566 and institutional start-up funds from Rutgers (to S.S.Y.) and financial support from Designs for Vision, Inc. The funders did not play a role in the study design, data collection and analysis, decision to publish, or preparation of the manuscript.

Ethics statement

This study did not include human samples. The use of human pathogens in the licensed BSL-2 laboratory was approved by the institutional biosafety committee. All biosafety regulations were followed during the conduct of this study.

Declaration of generative AI in scientific writing

The current version of ChatGPT (GPT-4o) was used to improve the readability and clarity in the abstract and introductory sections of this paper. The authors declare that generative AI was not used for scientific writing or in creating figures or images included in the manuscript.

CRediT authorship contribution statement

Junhong Sun: Data curation, Investigation, Validation. Sangeevan Vellappan: Data curation, Visualization, Writing- Original draft preparation. Johnathan Akdemir: Data curation, Visualization. Liviu Steier: Methodology, Resources. Richard E. Feinbloom: Methodology, Resources. Srujana S. Yadavalli: Conceptualization, Funding acquisition, Supervision, Writing- Original draft preparation, Writing- Reviewing and Editing.

Declaration of competing interest

The authors J.S., S.V., J. A., declare no competing interests. S.S.Y. collaborates with Designs for Vision, Inc. R.E.F. is the President Designs for Vision, Inc., and L.S. holds IP rights and receives royalties on Reveal.

Data Availability Statement

The authors declare that all data supporting the findings of this study are available within the main article and its supplementary information files.

References

1. Monika P, Chandraprabha MN, Rangarajan A, Waiker PV, Chidambara Murthy KN. 2021. Challenges in Healing Wound: Role of Complementary and Alternative Medicine. Front Nutr 8:791899.

2. Leaper D, Assadian O, Edmiston CE. 2015. Approach to chronic wound infections. Br J Dermatol 173:351–358.

3. Gardner SE, Hillis SL, Frantz RA. 2009. Clinical signs of infection in diabetic foot ulcers with high microbial load. Biol Res Nurs 11:119–128.

350 4. Eke PI, Dye BA, Wei L, Thornton-Evans GO, Genco RJ, CDC Periodontal Disease
351 Surveillance workgroup: James Beck (University of North Carolina, Chapel Hill, USA),
352 Gordon Douglass (Past President, American Academy of Periodontology), Roy Page
353 (University of Washin. 2012. Prevalence of periodontitis in adults in the United States: 2009
354 and 2010. J Dent Res 91:914–920.

355 5. Aydın SY, Ercan A, Ercan D. 2023. Investigation of the effects of clinical parameters on
356 mortality in patients with necrotizing fasciitis. Ulus Travma Acil Cerrahi Derg 29:1150–1157.

357 6. Ahluwalia RS, Reichert ILH. 2021. Surgical management of the acute severely infected
358 diabetic foot - The “infected diabetic foot attack”. An instructional review. J Clin Orthop
359 Trauma 18:114–120.

360 7. Avershina E, Khezri A, Ahmad R. 2023. Clinical Diagnostics of Bacterial Infections and
361 Their Resistance to Antibiotics-Current State and Whole Genome Sequencing
362 Implementation Perspectives. Antibiotics (Basel) 12.

363 8. Jones LM, Dunham D, Rennie MY, Kirman J, Lopez AJ, Keim KC, Little W, Gomez A,
364 Bourke J, Ng H, DaCosta RS, Smith AC. 2020. In vitro detection of porphyrin-producing
365 wound bacteria with real-time fluorescence imaging. Future Microbiol 15:319–332.

366 9. Lopez AJ, Jones LM, Reynolds L, Diaz RC, George IK, Little W, Fleming D, D’souza A,
367 Rennie MY, Rumbaugh KP, Smith AC. 2021. Detection of bacterial fluorescence from in
368 vivo wound biofilms using a point-of-care fluorescence imaging device. Int Wound J
369 18:626–638.

370 10. Shakibaie F, Lamard L. 2018. Application of fluorescence spectroscopy for microbial
371 detection to enhance clinical investigations. Photon Counting.

372 11. Koenig K, Schneckenburger H, Hemmer J, Tromberg BJ, Steiner RW. 1994. In-vivo
373 fluorescence detection and imaging of porphyrin-producing bacteria in the human skin and
374 in the oral cavity for diagnosis of acne vulgaris, caries, and squamous cell carcinoma, p.
375 129–138. *In* Advances in Laser and Light Spectroscopy to Diagnose Cancer and Other
376 Diseases. SPIE.

377 12. Choby JE, Skaar EP. 2016. Heme Synthesis and Acquisition in Bacterial Pathogens. J Mol
378 Biol 428:3408–3428.

379 13. Layer G. 2021. Heme biosynthesis in prokaryotes. Biochim Biophys Acta Mol Cell Res
380 1868:118861.

381 14. Gadberry JL, Amos MA. 1986. Comparison of a new commercially prepared porphyrin test
382 and the conventional satellite test for the identification of Haemophilus species that require
383 the X factor. J Clin Microbiol 23:637–639.

384 15. Lennon ÁM, Brune L, Techert S, Buchalla W. 2023. Fluorescence Spectroscopy Shows
385 Porphyrins Produced by Cultured Oral Bacteria Differ Depending on Composition of Growth
386 Media. Caries Res 57:74–86.

387 16. Gouterman M. 1961. Spectra of porphyrins. J Mol Spectrosc 6:138–163.

388 17. Case N, Johnston N, Nadeau J. 2024. Fluorescence microscopy with deep UV, near UV,
389 and visible excitation for in situ detection of microorganisms. Astrobiology 24:300–317.

390 18. Schalk IJ, Guillon L. 2013. Pyoverdine biosynthesis and secretion in Pseudomonas
391 aeruginosa: implications for metal homeostasis. Environ Microbiol 15:1661–1673.

392 19. Le L, Baer M, Briggs P, Bullock N, Cole W, DiMarco D, Hamil R, Harrell K, Kasper M, Li W,
393 Patel K, Sabo M, Thibodeaux K, Serena TE. 2021. Diagnostic Accuracy of Point-of-Care

394 Fluorescence Imaging for the Detection of Bacterial Burden in Wounds: Results from the
395 350-Patient Fluorescence Imaging Assessment and Guidance Trial. Adv Wound Care
396 10:123–136.

397 20. Schneider CA, Rasband WS, Eliceiri KW. 2012. NIH Image to ImageJ: 25 years of image
398 analysis. Nat Methods 9:671–675.

399 21. Teixeira R, Serra VV, Botequim D, Paulo PMR, Andrade SM, Costa SMB. 2021.
400 Fluorescence Spectroscopy of Porphyrins and Phthalocyanines: Some Insights into
401 Supramolecular Self-Assembly, Microencapsulation, and Imaging Microscopy. Molecules
402 26.

403 22. Granick S, Beale SI. 1978. Hemes, chlorophylls, and related compounds: biosynthesis and
404 metabolic regulation. Adv Enzymol Relat Areas Mol Biol 46:33–203.

405 23. Orlandi VT, Martegani E, Bolognese F, Trivellin N, Garzotto F, Caruso E. 2021.
406 Photoinactivation of Pseudomonas aeruginosa Biofilm by Dicationic Diaryl-Porphyrin. Int J
407 Mol Sci 22.

408 24. Ahle CM, Feidenhansl C, Brüggemann H. 2023. Cutibacterium acnes. Trends Microbiol
409 31:419–420.

410 25. Lemos JA, Palmer SR, Zeng L, Wen ZT, Kajfasz JK, Freires IA, Abranches J, Brady LJ.
411 2019. The Biology of Streptococcus mutans. Microbiol Spectr 7.

412 26. Condorelli F, Scalia G, Calì G, Rossetti B, Nicoletti G, Lo Bue AM. 1998. Isolation of
413 Porphyromonas gingivalis and detection of immunoglobulin A specific to fimbrial antigen in
414 gingival crevicular fluid. J Clin Microbiol 36:2322–2325.

415 27. Nakayama K. 2015. Porphyromonas gingivalis and related bacteria: from colonial
416 pigmentation to the type IX secretion system and gliding motility. J Periodontal Res 50:1–8.

417 28. Gera K, McIver KS. 2013. Laboratory growth and maintenance of Streptococcus pyogenes
418 (the Group A Streptococcus, GAS). Curr Protoc Microbiol 30:9D.2.1-9D.2.13.

419 29. Pierson LS 3rd, Pierson EA. 2010. Metabolism and function of phenazines in bacteria:
420 impacts on the behavior of bacteria in the environment and biotechnological processes.
421 Appl Microbiol Biotechnol 86:1659–1670.

422 30. Williams GJ, Al-Baraikan A, Rademakers FE, Ciravegna F, van de Vosse FN, Lawrie A,
423 Rothman A, Ashley EA, Wilkins MR, Lawford PV, Omholt SW, Wisløff U, Hose DR, Chico
424 TJA, Gunn JP, Morris PD. 2023. Wearable technology and the cardiovascular system: the
425 future of patient assessment. Lancet Digit Health 5:e467–e476.

426 31. Mondal S, Zehra N, Choudhury A, Iyer PK. 2021. Wearable Sensing Devices for Point of
427 Care Diagnostics. ACS Appl Bio Mater 4:47–70.

428 32. McKnight RR, Pean CA, Buck JS, Hwang JS, Hsu JR, Pierrie SN. 2020. Virtual Reality and
429 Augmented Reality-Translating Surgical Training into Surgical Technique. Curr Rev
430 Musculoskelet Med 13:663–674.

431 33. Barteit S, Lanfermann L, Bärnighausen T, Neuhann F, Beiersmann C. 2021. Augmented,
432 Mixed, and Virtual Reality-Based Head-Mounted Devices for Medical Education:
433 Systematic Review. JMIR Serious Games 9:e29080.

434 34. Cavallaro G, Decaria L, Rosato A. 2008. Genome-based analysis of heme biosynthesis and
435 uptake in prokaryotic systems. J Proteome Res 7:4946–4954.

436 35. Steier L, Sidhu P, Qasim SS, Mahdi SS, Daood U. 2022. Visualization of initial bacterial
437 colonization on dentin using fluorescence activating headlight for fluorescence enhanced
438 theragnosis. Photodiagnosis Photodyn Ther 38:102732.

439 36. Kornitzer D, Roy U. 2020. Pathways of heme utilization in fungi. Biochim Biophys Acta Mol
440 Cell Res 1867:118817.

441 37. Slimani A, Terrer E, Manton DJ, Tassery H. 2020. Carious lesion detection technologies:
442 factual clinical approaches. Br Dent J 229:432–442.

443 38. Steier L. 2020. Reveal: Fluorescence Enhanced Theragnosis by Designs for Vision. Eur J
444 Dent 14:186–188.

445 39. Steier L, Figueiredo JAP de, Blatz MB. 2021. Fluorescence-enhanced theragnosis: A novel
446 approach to visualize, detect, and remove caries. Compend Contin Educ Dent 42:460–465.

447 40. Hiltch G, Steier L, de Figueiredo JAP. 2023. Enhanced clinical decision-making and
448 delivery of minimally invasive care using the ICCMS4D integrated with hands-free
449 fluorescence-based loupes and a chemomechanical caries removal agent. Eur J Dent
450 17:1356–1362.

451
452
453
454
455
456
457
458

459 ## Tables, figures, and legends

460 **Table 1. List of bacterial and fungal strains plated on Porphyrin Test Agar (PTA) or blood**

461 **agar (BA) and tested for fluorescence production.**

Strain	Category	Growth	Incubation time in days	Fluorescence	
				PTA	BA
Gram-positive bacteria					
Corynebacterium minutissimum	skin	aerobic	5	Red/orange	Pink
Cutibacterium acnes (previously *Propionibacterium acnes*)	skin	anaerobic	10	Red	Red
Staphylococcus aureus	skin	aerobic	5	Red	−
Staphylococcus aureus (ΔhemB)		aerobic	5	−	−
Streptococcus mutans	oral	aerobic	5	−	−
		anaerobic	10	−	−
Listeria monocytogenes	other (blood)	aerobic	5	Red	−
Streptococcus pyogenes	other (respiratory tract)	anaerobic	10	Red	Red
		aerobic	5	−	−
Gram-negative bacteria					

Aeromonas hydrophila	skin	aerobic	5	Red	Pink
Pseudomonas aeruginosa	skin, multi-site	aerobic	5	Red	Cyan
Serratia marcescens	skin, urinary tract	aerobic	5	Red	Pink
Vibrio vulnificus	skin	aerobic	5	Red	Pink
Porphyromonas gingivalis	oral	anaerobic	10	Red	Red/black
Escherichia coli	other (intestinal, urinary tract)	aerobic	5	Red	−
Klebsiella pneumoniae	other (multi-site)	aerobic	5	Red	−
Proteus mirabilis	other (urinary tract)	aerobic	5	Pink	Cyan
Salmonella typhimurium	other (intestinal tract)	aerobic	5	Red	−
Fungi					
Candida albicans	skin	aerobic	10	−	−
Malassezia furfur	skin	aerobic	10	−	−

462

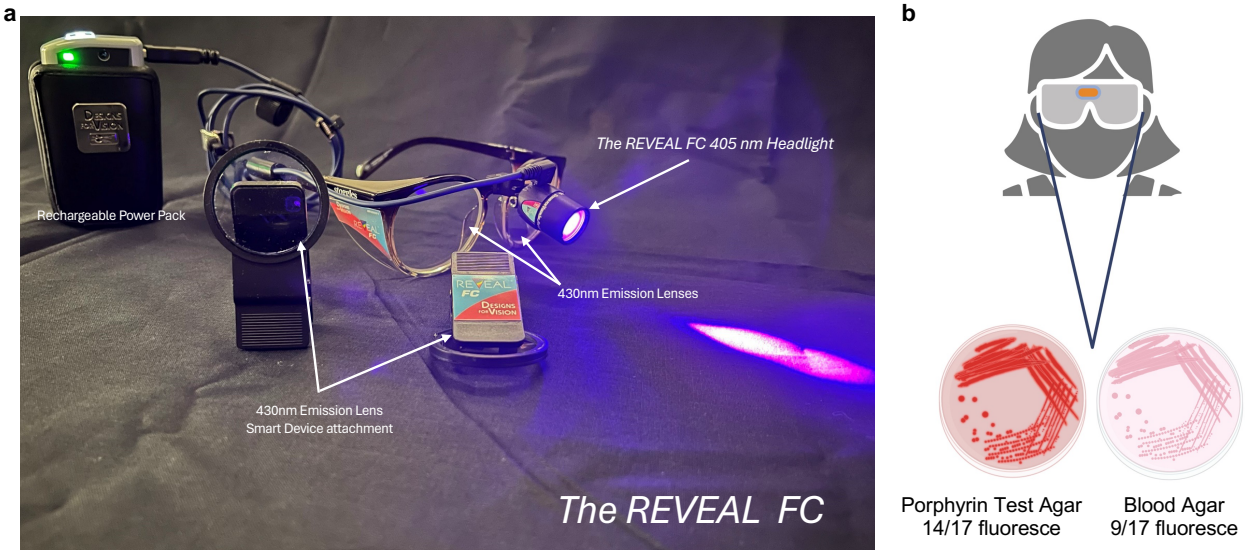

Figure 1. Overview of porphyrin-specific fluorescence detection in pathogenic microbes using the REVEAL FC imaging system. a) The REVEAL FC is a wearable imaging system composed of a headlight that provides excitation at 405 nm and observational eyewear, which includes the emission filter at 430 nm. This system includes a rechargeable power pack and smart device attachment for simple and effective visualization and imaging of microbial samples. b) 17 microbial species (15 bacteria and 2 fungi) commonly associated with skin, oral, and other infections were tested for autofluorescence of porphyrins. 14 of them exhibited fluorescence in shades ranging from red/orange to pink on porphyrin test agar, while 9 of them displayed fluorescence on blood agar.

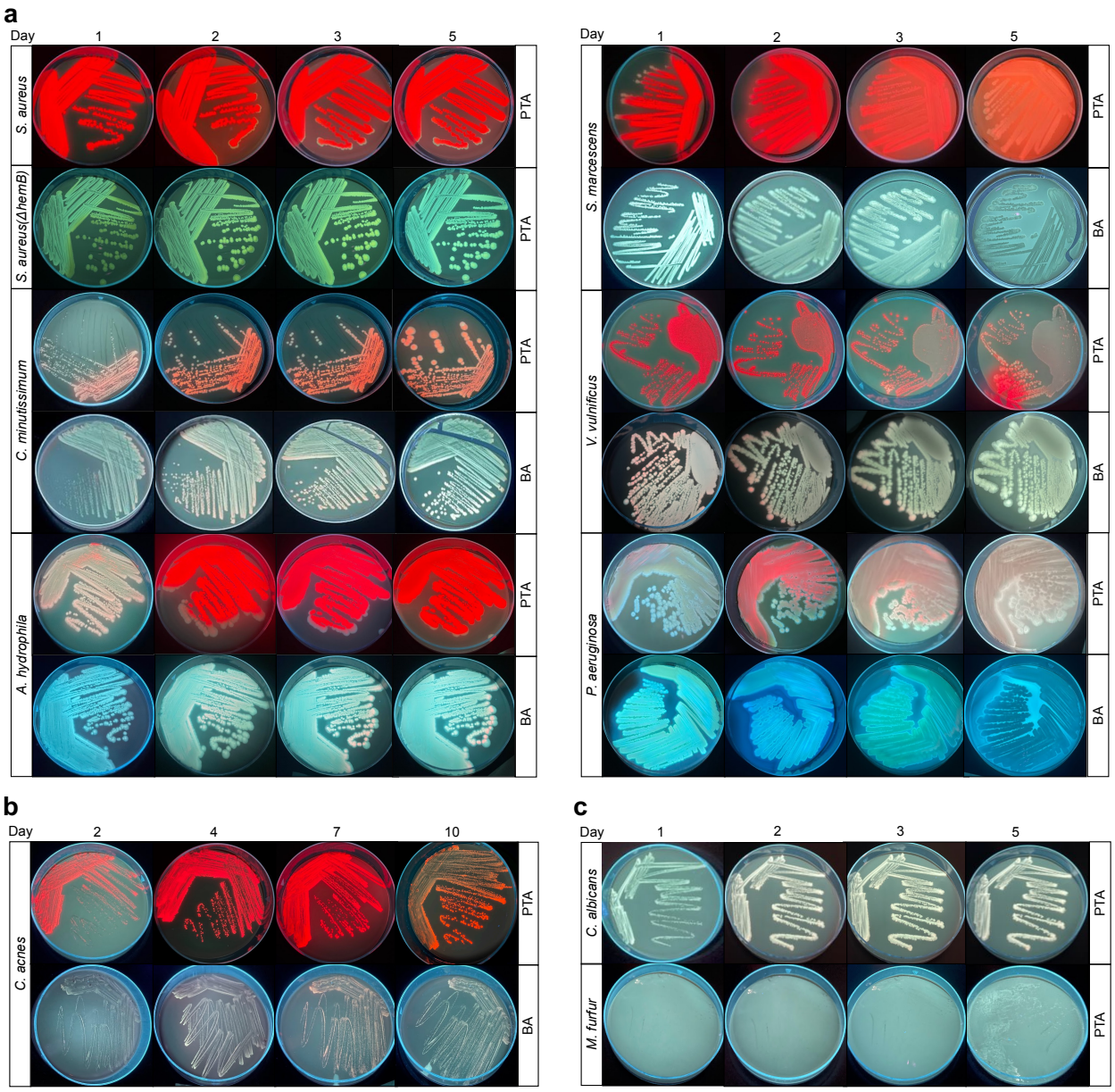

Figure 2. Porphyrin-specific fluorescence detection in microbes associated with skin infection. a) Fluorescence-based imaging of bacteria on porphyrin test agar (PTA) and/or blood agar under aerobic conditions after 1, 2, 3, and 5 days of growth. Bacterial strains *Staphylococcus aureus* and its mutant *ΔhemB*, *Corynebacterium minutissimum*, *Aeromonas hydrophila*, *Serratia marcescens*, *Vibrio vulnificus*, and *Pseudomonas aeruginosa* are labeled as *S. aureus*, *S. aureus ΔhemB*, *C. minutissimum*, *A. hydrophila*, *S. marcescens*, *V. vulnificus*, and

484 *P. aeruginosa*, respectively. b) Fluorescence-based imaging of bacteria grown on porphyrin test
485 agar (PTA) and/or blood agar under anaerobic conditions after 2, 4, 7, and 10 days of growth.
486 The bacterial strain *Cutibacterium acnes* is labeled as *C. acnes*. c) Fluorescence-based imaging
487 of fungi on porphyrin test agar (PTA) and/or blood agar under aerobic conditions after 1, 2, 3,
488 and 5 days of growth. Fungal strains *Candida albicans* and *Malassezia furfur* are labeled as *C.*
489 *albicans* and *M. furfur*, respectively. Images are representative of four biological replicates.
490
491
492
493
494
495
496

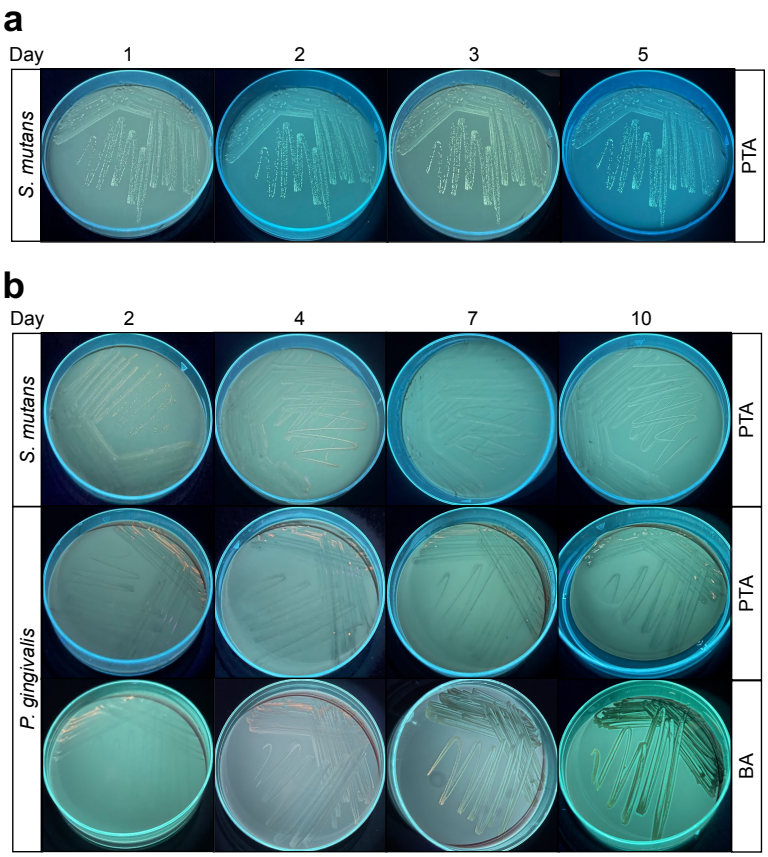

Figure 3. Porphyrin-specific fluorescence detection in bacteria associated with oral infection. a) Fluorescence-based imaging of bacteria on porphyrin test agar (PTA) and/or blood agar under aerobic conditions after 1, 2, 3, and 5 days of growth. The bacterial strain *Streptococcus mutans* is labeled as *S. mutans*. b) Fluorescence-based imaging of bacteria grown on porphyrin test agar (PTA) and/or blood agar under aerobic conditions after 2, 4, 7, and 10 days of growth. Bacterial strains *Streptococcus mutans* and *Porphyromonas gingivalis* are labeled as *S. mutans* and *P. gingivalis*, respectively. Images are representative of four biological replicates.

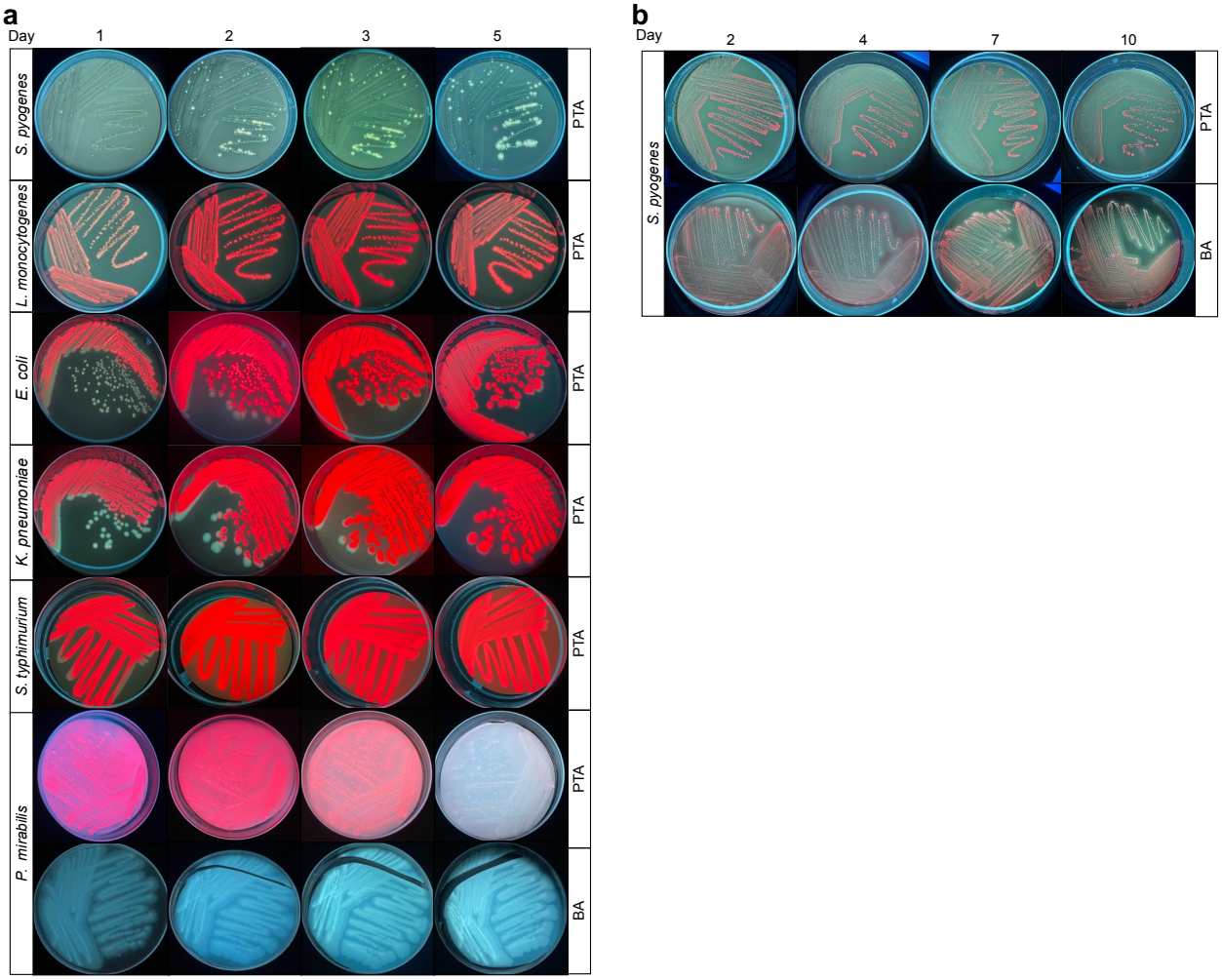

509

510

511 **Figure 4. Porphyrin-specific fluorescence detection in bacteria associated with other**

512 **infections.** a) Fluorescence-based imaging of bacteria on porphyrin test agar (PTA) and/or

513 blood agar under aerobic conditions after 1, 2, 3, and 5 days of growth. Bacterial strains

514 *Streptococcus pyogenes*, *Listeria monocytogenes*, *Escherichia coli*, *Klebsiella pneumoniae*,

515 *Salmonella typhimurium*, and *Proteus mirabilis* are labeled as *S. pyogenes*, *L. monocytogenes*,

516 *E. coli*, *K. pneumoniae*, *S. typhimurium*, and *P. mirabilis*, respectively. b) Fluorescence-based

517 imaging of bacteria grown on porphyrin test agar (PTA) and/or blood agar under aerobic

518 conditions after 2, 4, 7, and 10 days of growth. The bacterial strain *Streptococcus pyogenes* is

519 labeled as *S. pyogenes*. Images are representative of four biological replicates.

520 ## Supporting Information

521 **Table S1. List of strains, growth conditions, and liquid culture media used in the study.**

522

Strain	Growth condition and media	Source
Bacteria		
Aeromonas hydrophila	aerobic, 37ºC, Tryptic Soy Broth (Avantor)	ATCC 35654
Corynebacterium minutissimum	aerobic, 37ºC, Brain Heart Infusion (BD)	ATCC 23348
Cutibacterium acnes (previously *Propionibacterium acnes*)	anaerobic, 37ºC, Tryptic Soy Broth (Avantor)	ATCC 6919
Escherichia coli MG1655	aerobic, 37ºC, LB Miller (IBI Scientific)	Yadavalli lab
Klebsiella pneumoniae 13883	aerobic, 37ºC, LB Miller (IBI Scientific)	Fan lab
Listeria monocytogenes	aerobic, 37ºC, Brain Heart Infusion (BD)	ATCC 19115
Porphyromonas gingivalis	anaerobic, 37ºC, Tryptic Soy Broth (Avantor), supplemented with Vitamin K and hemin (BD)	ATCC 33277
Proteus mirabilis	aerobic, 37ºC, LB Miller (IBI Scientific)	ATCC 25933
Pseudomonas aeruginosa PAO1	aerobic, 37ºC, LB Miller (IBI Scientific)	Nickels lab
Salmonella typhimurium 14028	aerobic, 37ºC, LB Miller (IBI Scientific)	Schifferli lab
Serratia marcescens	aerobic, 37ºC, LB Miller (IBI Scientific)	ATCC 13880

Staphylococcus aureus USA300_LAC (community acquired MRSA strain)	aerobic, 37ºC, LB Miller (IBI Scientific)	Boyd lab
Staphylococcus aureus (ΔhemB)	aerobic, 37ºC, LB Miller (IBI Scientific)	Boyd lab
Streptococcus mutans	aerobic, 37ºC, Brain Heart Infusion (BD)	ATCC 35668
	anaerobic, 37ºC, Brain Heart Infusion (BD)	
Streptococcus pyogenes	aerobic, 37ºC, Brain Heart Infusion (BD)	ATCC 19615
	anaerobic, 37ºC, Brain Heart Infusion (BD)	
Vibrio vulnificus	aerobic, 37ºC, LB Miller (IBI Scientific)	ATCC 27562
Fungi		
Candida albicans	aerobic, 37ºC, Yeast Peptone Dextrose Broth (BD)	ATCC 18804
Malassezia furfur	aerobic, 37ºC, Brain Heart Infusion (BD) supplemented with Ox bile (Hardy Diagnostic)	ATCC 14521

523

a Transmission curve of a 405 nm LED

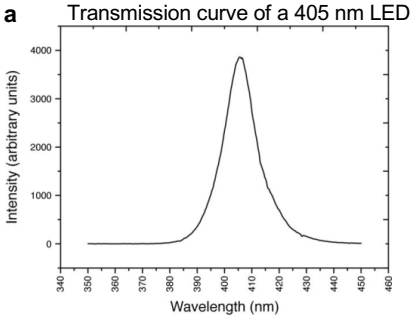

b Transmission curve of REVEAL FC

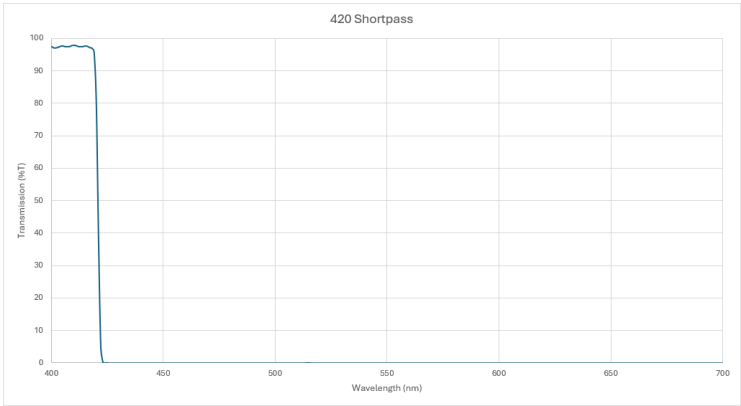

c

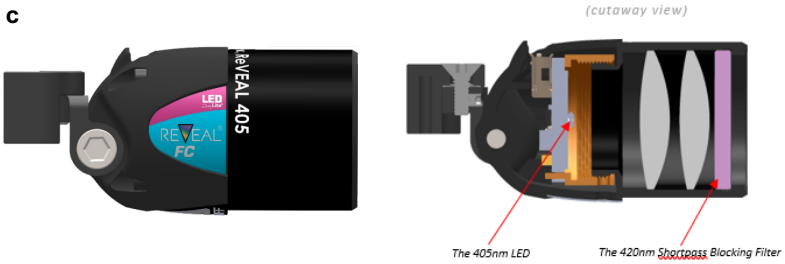

d Emission curve of REVEAL FC

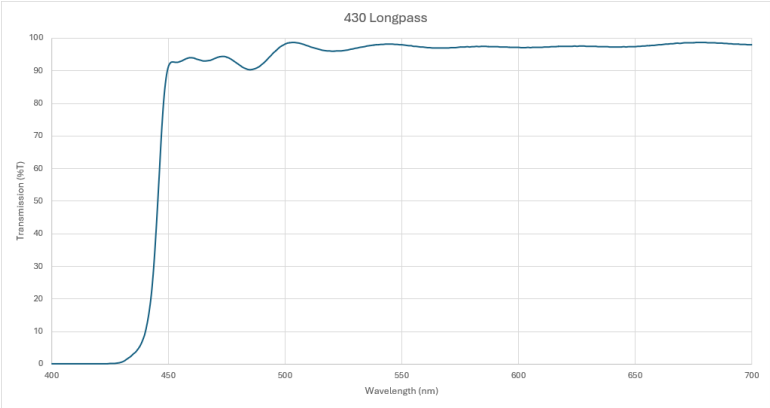

526 **Figure S1. Fluorescence emission spectra for the 405 nm LED.** a) Representative
527 transmission curve of a typical 405 nm LED showing light transmission across a range of
528 wavelengths (380 – 450 nm). b) Transmission curve of REVEAL FC using a 420 nm shortpass
529 filter focusing fluorescence excitation at 400 – 425 nm. c) Diagram of the REVEAL FC lens with
530 a cross-sectional depiction of the 405 nm LED and the 420 nm shortpass cut-off filter. d)
531 Emission curve of REVEAL FC lens showing emission at wavelengths ≥ 430 nm.